CrystEngComm

Accepted Manuscript

ROYAL SOCIETY OF CHEMISTRY

www.rsc.org/crystengcomm

Cite this: DOI: 10.1039/c0xx00000x

www.rsc.org/xxxxxx

ARTICLE TYPE

Bis(paracetamol) pyridine – a new elusive paracetamol solvate. From modeling the phase diagram to successful single-crystal growth and structure-property relations

Boris A. Zakharov, [a,b] Andrey G. Ogienko, [b,c] Alexander S. Yunoshev, [b,d] Alexey I. Ancharov, [a,b,c] Elena V. Boldyreva*[,a,b]

Received (in XXX, XXX) Xth XXXXXXXXX 20XX, Accepted Xth XXXXXXXXX 20XX
DOI: 10.1039/b000000x

Multi-component crystals – salts, co-crystals, or solvates - are usually designed based on the analysis of complementarity of functional groups and intermolecular interactions of the components. However, no *crystal design* can do without a practical method of *crystal growth*. Not all compounds that should be expected to exist based on the "synthon approach" can be prepared in real experiments. This paper aims to illustrate that, in addition to the synthon approach, it is equally important to take into account phase diagrams when searching for practical methods of crystallising multi-component crystals, either as single crystals or as fine particles. Here, we describe the crystallization of *bis*(paracetamol) pyridine solvate from a glass-like metastable phase produced by quench-freezing of the paracetamol-pyridine solution with subsequent low-temperature annealing. These procedures must be carried out strictly within the boundaries of the two-phase region "solid solvate + liquor", which was found only as a result of modelling the phase diagram. The crystal structure was solved by single-crystal X-ray diffraction and compared with co-crystals of paracetamol found in Cambridge Structural Database. The structure-forming role of the intermolecular interactions and their characteristics were studied by variable-temperature experiments over the range of 100-275 K. This was compared with the structures of pure paracetamol polymorphs and other solvates and co-crystals at ambient and non-ambient conditions.

Introduction

Crystal engineering is a rapidly developing field[1–5] and the design of desirable crystal structure with target properties is important for materials sciences and drug development[5–13]. Quite often a structure is formed by more than one component. One of the main principles of designing a multi-component crystal is selecting co-formers with complementary functional groups, molecular shapes and sizes[4,14–19]. However, no *crystal design* can do without an experimental method for *crystal growth*. Obtaining a multicomponent crystal remains a challenge even if all the requirements of molecular shape, size and complementarity of functional groups are fulfilled. Crystallisation is traditionally used to purify compounds and to crystallise components selectively as pure phases from multicomponent mixtures, be they solutions or melts[20–24]. To achieve an opposing aim, *i.e.* to co-crystallise several components in one solid phase, one needs to know the thermodynamics and kinetics of the process[25–28]. Some multicomponent crystals are thermodynamically less favourable than a mixture of pure phases of the individual components. In such cases, the multicomponent crystals can be obtained under non-equilibrium conditions only, such as rapid precipitation by anti-solvents, spray-drying, or by co-grinding[5,29–36]. In other cases, the target multicomponent crystal is thermodynamically stable, but the components as solid phases differ so much in melting temperatures or in solubilities, that it is very difficult to find a practical method of co-crystallising them into a single phase. Careful preliminary studies of the phase diagrams in such systems are required in order to reliably control the crystallisation process. For example, detailed studies of the solubility curves for all components make it possible to get co-crystals by crystallisation from multicomponent solutions even if the solubilities of components differ significantly[26,27,37]. Phase diagrams are helpful to optimize co-crystallisation conditions, to obtain co-crystals from the melt or solution, or by spray-drying[38–42]. Attempts are also known in which phase diagrams are applied to predict the result of co-grinding component mixtures[43,44], although it was shown in several papers that the products of co-grinding, more often than not, correspond to non-equilibrium conditions[33,45–48].

Paracetamol is one of the compounds that is widely used as a model in many respects, in particular for the study of polymorphism[49–51], intermolecular interactions[51–53], intramolecular motions of selected groups[54–57]and co-crystal or solvate formation[58–66]. Crystal structures of 30 multicomponent crystals of paracetamol including co-crystals, salts and solvates, have been deposited in Cambridge Structural Database (version 5.35 from November 2013[67]). Strangely enough, a solvate of

paracetamol with pyridine has never been reported until now, though pyridine could be expected to form hydrogen bonds with paracetamol, and the size and shapes of the molecules of each compound should also match. Paracetamol both interacts with and is soluble in pyridine. For example, the shapes of etch pits formed on bringing the surface of the single crystals of paracetamol into contact with liquid pyridine or pyridine vapour were studied[68]. Apart of the general interest of pyridine as a common co-former for many organic multicomponent crystals, the study of its solvate with paracetamol may be interesting with the aim of a better understanding of the mechanisms of paracetamol hepatotoxicity and for the design of new forms of drugs based on paracetamol and related compounds. For example, in medicinal chemistry paracetamol analogues with pyridinol-fused rings were shown to be more metabolically stable and exhibit less direct cytotoxicity as compared with paracetamol. Such analogues are leading candidates for studies to determine whether they are free of the metabolism-based hepatotoxicity produced by acetaminophen[69]. Pyridine and pyrimidine analogues of paracetamol act as inhibitors of lipid peroxidation and cyclooxygenase and lipoxygenase catalysis[70]. Though there is an enormous difference between paracetamol analogues with pyridine-fused rings and a paracetamol / pyridine solvate, knowledge of the properties of hydrogen bonds formed between the pyridine and the acetaminophen fragments in a crystal is important to understand the behaviour of these species in solution. Further, this knowledge can assist in rationalising interactions with receptors in the body, a prevailing issue despite more than a century of research[71].

Attempts to obtain a pyridine solvate of paracetamol by ''trial and error'' through a direct method, i.e. bringing paracetamol in contact with pyridine and varying experimental conditions (temperature, concentration, additional solvent) failed. This system has therefore been selected for a case study in order to understand why a co-crystallisation can fail, even when two relatively small and simple molecules should form co-crystals according to molecular shapes, sizes and the presence of complementary hydrogen bond donors and acceptors. We could suggest that the two components would not co-crystallise unless a rather narrow temperature and concentration range was selected. To overcome these difficulties it was necessary to study and use the phase diagram of the system.

The aims of the present study were thus to find the conditions for the co-crystallisation of paracetamol and pyridine using the phase diagram, to solve the crystal structure of the target multicomponent crystal, to analyse molecular packing, molecular conformations and intermolecular interactions in the crystal structure and compare with the pure polymorphs of paracetamol. This example can be followed to obtain other solvates and co-crystals when similar crystallisation problems occur.

Materials and Methods

Several steps were undertaken, to find conditions of crystallising the target solvate. Preliminary solubility tests were followed by flash-freezing of paracetamol in a pyridine solution (hereafter "frozen solution") and its subsequent heating under variable conditions, in order to find the conditions of the existence and co-existence of different solid and liquid phases in the system. The solid phases formed in the system were identified by analysing powder diffraction patterns collected using synchrotron radiation. Details of the experiments are deposited as ESI (ESI, Part I). After conditions for growing single crystals of a paracetamol – pyridine solvate were found, the crystal structure was solved and refined at multiple temperatures. Details of the data collection and refinement, as well as of crystal structure analysis are also deposited as ESI (ESI, Part III). Complete structural data were deposited in the CSD[67] with refcodes CCDC 816885 – 816892.

Results and Discussion

Phase diagram and crystallisation conditions

Attempts to obtain a paracetamol-pyridine solvate in a straightforward way by direct crystallisation failed. Heating of paracetamol-pyridine mixtures with a paracetamol content of 20 and 40 wt. % (i.e., 11.6 and 25.9 mol %, respectively) to 330 K resulted in complete dissolution of paracetamol; however no precipitation was observed after subsequent cooling to room temperature (or lower). A precipitate of pure monoclinic paracetamol powder (as revealed by X-ray diffraction analysis) was the only solid phase observed after partial pyridine evaporation. The samples with higher paracetamol content (50, 60 and 80 wt. %, or 34.3, 44.0, 67.7 mol %, respectively) did not dissolve completely, even on heating to 330 K (or slightly higher) and stirring for several hours. After the mixtures were equilibrated for several weeks, the precipitates were taken for XRD analysis and confirmed to consist exclusively of pure monoclinic paracetamol without impurities of other phases.

Our previous experience has shown that flash-freezing the solutions with subsequent annealing can be helpful for obtaining phases that are difficult to otherwise crystallise. For example, the crystalline X-phase of glycine can only be obtained by low-temperature annealing of a metastable glass formed from quench-freezing of an aqueous solution[72]. This phase transforms into β-glycine almost immediately after being formed, and can only be preserved at significantly lower temperatures.

Preliminary diffraction experiments revealed the formation of amorphous glassy phases (no reflections were present in the powder diffraction patterns) on quench-freezing of the paracetamol solutions in pyridine to below the pyridine melting point. New reflections appeared when the sample was warmed to 243 – 275 K, which could not be assigned to any of the known paracetamol polymorphs. At temperatures above 277 K the reflections of this new phase disappeared due to its dissolution (see examples of powder patterns in the ESI, Fig. S1)).

Further diffraction experiments were carried out using a low-temperature TTK 450 Anton Paar chamber, which allowed work under reduced pressure. The sample was placed into the holder at 140 K, the temperature was raised to 235 K, after which the reflections of the new phase appeared. The presence of a liquid phase could be observed by eye and also manifested in a higher background of the powder diffraction pattern collected at this temperature. Decreasing the pressure in the chamber, whilst maintaining the sample at 260 K, resulted in removal of pyridine from the liquid phase by evaporation. As the temperature increased further at low pressure ($P < 5 \cdot 10^{-2}$torr), the reflections corresponding to the monoclinic polymorph of paracetamol

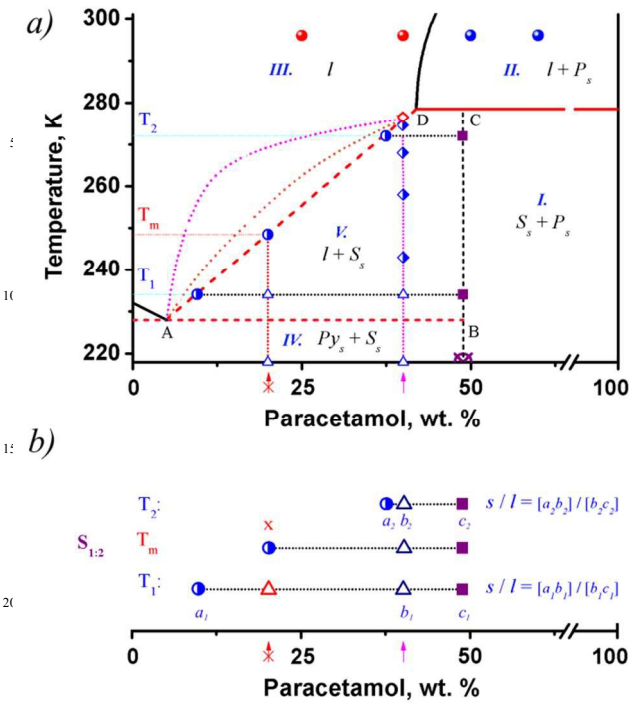

Figure 1. Selecting the conditions for obtaining the paracetamol-pyridine solvate crystal suitable for single-crystal X-ray diffraction. (a) Estimated composition of paracetamol-pyridine solvate (1:2) shown as crossed purple circle. Designations: Py – pyridine; P – paracetamol; S – paracetamol – pyridine solvate; l – liquor; s – solid phase. Data on solubility of paracetamol in pyridine are shown as red circles (one-phase region: liquor) and blue circles (two-phase region: "paracetamol(solid phase) + liquor"). The results of the diffraction experiments are shown as a half-filled blue rhombus (two-phase region: "solvate(solid phase) + liquid phase") and a red rhombus (one-phase region: liquor). (b) An illustration of the principle behind the selection of the optimal paracetamol concentration. Example of solvates with highest pyridine content (paracetamol : pyridine = 1:2, S1:2), with changes in the ratios of the liquid phase and resulting solvate crystals at different temperatures shown in real scale based on Fig. 1a. Designations: T1 and T2 – minimum and maximum allowed crystallisation temperature; liquid phase - half-filled blue circles; purple square – solid phase of estimated paracetamol – pyridine solvate; blue triangles – position of state point. Allowed concentration indicated by arrow, not-allowed – by crossed arrow; Tm – the melting temperature of the mixture with not-allowed concentration.

appeared, increasing in intensity. By 330 K the sample consisted exclusively of pure monoclinic paracetamol.

Thus, the paracetamol-pyridine solvate was easily obtained as a fine powder by low-temperature annealing of quench-frozen solutions. This compound was stable for only several minutes on air and, on further storage, was losing pyridine to give monoclinic paracetamol. In order to grow a single crystal suitable for single-crystal X-ray diffraction, it was necessary to find the *T*, *P* range in which the solvate coexisted with the liquid phase (stock solution). This could only be done by modelling the phase diagram (see ESI for further details, Fig. S2).

Experimental observations of phases in selected P,T regions allowed us to give preference to the variant of the phase diagram presented in Fig. 1.[i] The range over which crystallisation is possible ("solid solvate – liquor" field of the phase diagram) is represented by the rectangular trapezoid ABCD. In the absence of information on the paracetamol-pyridine solvate stoichiometry, the maximum permitted paracetamol concentration in the starting solution (before quench-freezing) was restricted to the composition of the solvate with the highest pyridine content (1:2). This ensured that the state point[ii] would remain in the two-phase region "solid solvate + liquor" and not move to the two-phase region "solid solvate + solid paracetamol" (region I). This is the upper concentration boundary. If the initial concentration of paracetamol in solution is consistent with the 1:2 solvate stoichiometry, i.e. in the range of ~40 - 49 wt. % (25.9 – 33.5 mol %), heating above 275 K (the highest temperature at which the unknown phase was observed in diffraction experiments) leads to crossing the peritectic line. Then the state point comes from the two-phase region "solid solvate + liquor" to the two-phase region "solid paracetamol + liquor" (region II), which is the equilibrium state under these conditions. In this case, the metastable state developed by quench-freezing would be lost, and a new experiment would be required to re-obtain it. This is the upper temperature boundary. If the initial concentration of paracetamol in solution is less than 40 wt. % (25.9 mol %), overheating leads to crossing the liquidus curve. Then the state point moves from the two-phase region "solid solvate + liquor" to the one-phase region of liquor (region III). In this case the metastable state achieved by quench-freezing will again be lost and a new experiment required to re-obtain it. Possible variants of the liquidus curve are shown as orange and magenta dotted lines. A maximum possible temperature dependence of the paracetamol concentration was estimated as ~1 K/wt.% (shown as red dashed line). [iii] Decrease in temperature below the eutectic line (region IV) leads to movement of the state point from the two-phase region "solid solvate + liquor" to the two-phase region "solid solvate + solid pyridine". In the case of an equilibrium state, crossing the eutectic line leads to the formation of small crystals and is not a problem for obtaining good quality single crystals. However in the case of the metastable state, crossing the eutectic line on freezing of the liquid phase of eutectic composition may

[i] Experimental observations are consistent with two variants (defined as *b* and *c* at Fig. S1 in ESI). The two-phase regions, "solid solvate + liquor," are the same for both models. Since the subsolidus region is of no interest for obtaining single crystals, for the sake of simplicity we considered only one variant (*b)* at Fig. S2 in ESI) when searching for optimum concentration and temperature ranges for successful single crystal growth.

[ii] State point is defined as a position on the phase diagram representing a specific set of state variables

[iii] The following assumptions were made: a) the eutectic temperature is very close to the melting point of pure pyridine (~230 K) and the peritectic temperature is not much above 275 K; b) the peritectic point is in the range of 40 and ~49 wt. % of paracetamol and the eutectic point is degenerated at less than 5 wt. % of paracetamol.

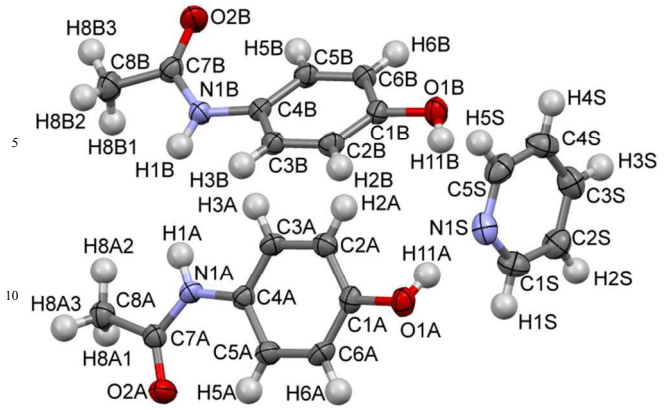

Figure 2. Displacement ellipsoid plot of bis(paracetamol) pyridine at 50% probability (T = 200 K) showing the atom numbering scheme.

lead to the formation of small crystals of monoclinic paracetamol, instead of those of the paracetamol-pyridine solvate. These nuclei will further act as nucleation centres for growth of large crystals of the stable phase of monoclinic paracetamol. This is the lower temperature boundary.

This analysis showed that the only possible way to obtain single crystals of the title solvate was by slow thawing of the quench-frozen sample to the eutectic point (pyridine$_{(solid)}$ + solvate$_{(solid)}$ = liquor), followed by multiple heating/cooling cycles within the boundaries of the two-phase region "solid solvate + liquor" (Fig. 1, Fig. S3).

Another issue was selecting the optimum starting concentration of paracetamol for this crystallisation strategy. The ratio of the phases should be considered at different temperatures between the minimum and the maximum allowed values (*i.e.* slightly above the eutectic (T_1) and slightly below the peritectic or liquidus curve (T_2)). This will reduce the influence of temperature control errors during the experiment, preventing inadvertent loss of the metastable state. The temperature borders of the trapezoid ABCD (the bases of the trapezoid) are limited by the eutectic and peritectic points. The composition border (the line normal to the trapezoid bases) is determined by the composition of the solvate with minimum possible pyridine content. These three borders are fixed and their characteristics (temperature / concentration) do not correlate with each other. The only variable border is the inclined side of the trapezoid (approximation of the liquidus curve). Its position depends on the temperature and concentration and are, in this case, interrelated: a change in temperature results in the corresponding change in concentration and *vice versa*. The slope of this side determines the phase ratio at different temperatures. One has to select between the easiness to manipulate with crystals and the possibility to maintain the required temperature gradient. Using lower concentrations of paracetamol in solution would make it easier to select and handle single crystals. However, in this case the temperature gradient in which crystallisation can take place without partial or complete melting, is significantly smaller. Dilute (20 wt. %, 11.6 mol %) solutions crystallise very reluctantly. The difference, ΔT, between the minimum temperature (eutectic T_1) and the maximum temperature (slightly below the liquidus curve), is, in this, case ~ 15 K, while the temperature T_2 can no longer be reached – everything will melt (Fig. 1a). This ΔT is smaller than the overcooling required for nucleation of the target phase. For comparison, the ΔT for a 40 wt. % sample is ~ 30 K. If a larger temperature gradient (T_2 - T_1) is used for recrystallisation of polycrystals into several larger single crystals, it is more difficult to handle the sample as the amount of mother liquor becomes smaller. For example, during the crystallisation process, the solid:liquid phase ratio changes from ~3/10 to ~30/10 for the solvate with highest pyridine content (1:2) (Fig.1, *b*) and from ~3/40 to ~30/40 for the solvate with lowest pyridine content (1:0.5) (Fig.S2). **As an acceptable compromise, the initial paracetamol concentration in solution was selected as 40 wt. %.**

Crystal structure analysis

As mentioned above, one of the aims of this study was to analyse molecular packing, molecular conformations and intermolecular interactions in the crystal structure of the paracetamol-pyridine solvate, comparing this to pure polymorphs of paracetamol.

An asymmetric unit of *bis*(paracetamol) pyridine contains two independent paracetamol molecules and one pyridine molecule (Fig. 2). An interesting feature of this structure is that two symmetrically independent paracetamol molecules have different conformations. Positions of the acetamide groups with respect to the aromatic rings can be characterized by torsional angles C5A-C4A-N1A-C7A and C5B-C4B-N1B-C7B. At 275 K these angles were found to be 1.0(3)º and 28.7(3)º, respectively (Fig. S4). The values of the C-C-N-C angles in different paracetamol-containing structures found in the CSD[67] vary from 1 to 49º. In pure paracetamol, with only one molecule in the asymmetric unit, paracetamol molecules are not flat, but remain less bent in the orthorhombic form[52] than in the monoclinic one[57]. According to quantum chemical calculations, an isolated paracetamol molecule should be flat, with any bent conformation resulting from its ionization[73]. In a crystal, conformational changes can result from (i) the intermolecular interactions with neighbouring molecules, in particular from partial ionization of potential hydrogen bond donors or acceptors[53,74], as well as from (ii) the conformational adjustment, aiming to optimise molecular packing[75].

The fragments of the crystal structures of *bis*(paracetamol) pyridine and individual paracetamol polymorphs are shown in Fig.3. The types of hydrogen bonds formed in *bis*(paracetamol) pyridine are very different from those in the polymorphs of pure paracetamol. Three types of hydrogen bonds are present, but none of them is the same as in pure paracetamol (Fig, 3, Table S2, ESI). In pure paracetamol polymorphs, the hydroxyl-groups act simultaneously as proton donors, linking to the -C=O groups of the acetamide fragments, and proton acceptors, accepting protons from the NH-groups of the acetamide fragments. The molecules are connected *via* the N-H...O and O-H…O bonds in the chains and then further into the 2D-layers[52,57]. Neither –NH…OH, nor –OH…O=C- bonds are formed in *bis*(paracetamol) pyridine. Amino-groups form "peptide" H-bonds to the O=C- groups, so that infinite chains of paracetamol molecules along the crystallographic *c* axis arise. The –OH groups still act simultaneously as proton donors and proton acceptors in hydrogen bonds, but in the solvate they donate protons either to the N-atoms of the pyridine molecules, or to other –OH groups, linking two paracetamol molecules from neighbouring chains along the crystallographic *a* axis. Flat and bent paracetamol

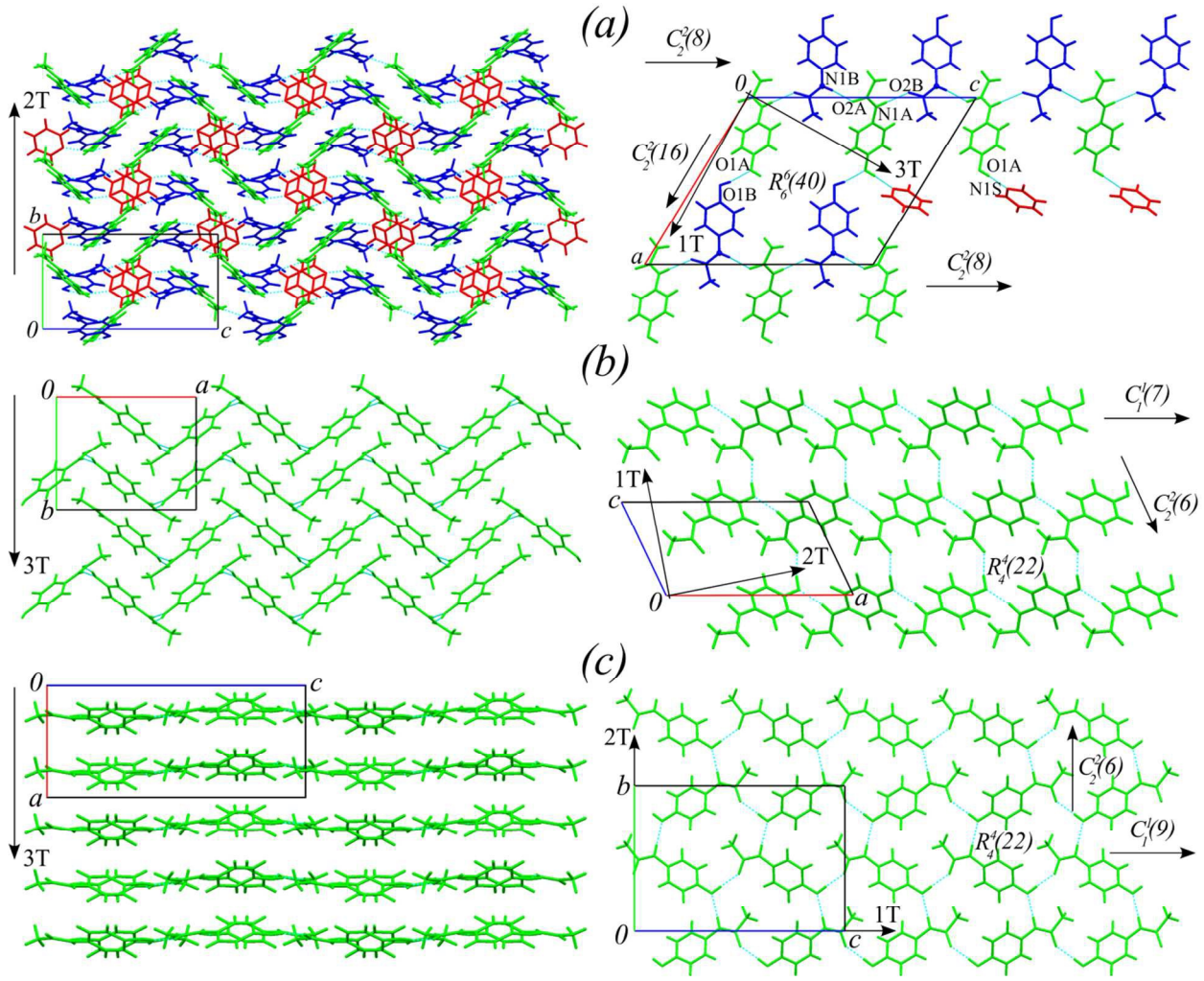

Figure 3. The fragments of crystal structures of *bis*(paracetamol) pyridine (a), and for comparison monoclinic (b) and orthorhombic (c) paracetamol. These show the main structural motifs, hydrogen bonds and directions of principal axes 1T, 2T, 3T of the strain ellipsoid on cooling, corresponding to minimum, medium and maximum compression, respectively [52,57]

molecules (linked to pyridine, or not, respectively) alternate in a chain. The -OH…OH hydrogen bond motif is common for alcohols[76,77] and was, for example, observed in L-serine,[78] among many other structures. The paracetamol molecules connected to each other by N-H...O and O-H...O hydrogen bonds form undulating layers consisting of $R_6^6(40)$ rings, and $C_2^2(8)$ chains. No hydrogen bonds between these layers are present. This network of hydrogen bonds is similar to those present in the crystal structures of other solvates[iv] of paracetamol with N,N'-dimethylpiperazine, N-methylmorpholine, piperazine, morpholine[79]. For comparison, the molecular layers formed by NH...OH and O-H...O=C hydrogen bonds are pleated in monoclinic paracetamol and flat in the orthorhombic polymorph. Each pyridine molecule is connected to a paracetamol molecule within the layer by an O-H...N hydrogen bond. Pyridine fills the gaps between the undulating layers formed by paracetamol to optimise molecular packing. It is the ability of paracetamol to form -OH…N bonds, that changes the general pattern of the H-bond network that connects paracetamol molecules, as compared with pure paracetamol polymorphs. The possibility to form infinite molecular chains linked by -NH…O=C- hydrogen bonds, together with the void-filling by pyridine molecules, can be suggested as the driving force for excluding -OH…O=C- bond formation. Interestingly, pyridine can compete for a proton with a stronger proton accepter: the oxygen atom of the acetamide group. This illustrates that a comparison of the strengths of the individual H-bonds can be misleading when trying to predict crystal packing, since the total lattice energy is a result of the interplay of a multitude of interactions. In several other two-component paracetamol solvates, in which the hydroxyl group of paracetamol can form H-bond with the nitrogen atom of a co-former molecule, paracetamol molecules also form infinite chains connected to each other by "peptide" -N-H...O=C- hydrogen bonds between acetamide groups (Fig.3a). Examples of this include 4,4'-Ethene-1,2-diyldipyridine (KETYUF)[80], trans-Cyclohexane-1,4-diamine (WIGCEW)[81], N,N'-dimethylpiperazine (MUPPIW), N-methylmorpholine (MUPPOC), piperazine (MUPPUI) and morpholine (MUPQET)[79].This fact is also of importance for understanding

[iv]Termed "co-crystals" in the original paper

the pharmacological action of paracetamol, showing that its phenol group can form H-bonds with N-atoms of heterocyclic compounds, even in the presence of a strongly competing proton acceptors such as the O=C- of an acetamido group.

Even though much knowledge of the interactions in a crystal structure can be gained from the analysis at ambient conditions only, following structural changes on cooling is even more informative[82–84]. Cooling *bis*(paracetamol) pyridine from 275 to 100 K did not result in any phase transitions, but anisotropy of strain gave a better insight into the relative strengths of different types of hydrogen bonds. Strain anisotropy on cooling was clearly correlated with the directions of molecular chains linked by different types of H-bonds (Table S2, Figs. S5 & S6 in ESI). Maximum compression was observed along the axes of undulating molecular bands ("accordion'' type compression, N1B-H1B...O2A (-x, -y+1, -z) and O1A-H11A...N1S hydrogen bonds) and minimum compression was observed in the molecular layers, normal to the band axes (N1A-H1A...O2B (-x, y+1/2, -z+1/2), O1B-H11B...O1A (-x+1, y-1/2, -z+1/2) hydrogen bonds). In *bis*(paracetamol) pyridine the relative orientation of paracetamol molecules changes. This makes an additional contribution to lattice strain on cooling and can explain why the maximum compression of this structure is observed along the axes of undulating molecular bands, rather than normal to the layers as in paracetamol polymorphs in which the layers themselves are more rigid[52,57].

Conclusions

Not all combinations of co-formers that might be expected to give multicomponent crystals based on analysis of the complementarity of functional groups and molecular sizes and shapes can be easily produced in real experiments. The present study serves as an illustration of the usefulness of a thermodynamic approach for finding the conditions under which target multi-component crystals can be obtained. The crystal structure of *bis*(paracetamol) pyridine shows several interesting features, including the co-existence of two independent paracetamol molecules in different conformations and the formation of three types of intermolecular hydrogen bonds, none of which is present in structures of the pure paracetamol polymorphs. The ability of paracetamol to form O-H…N bonds, complemented by void-filling pyridine molecules, changes the general pattern of the H-bond network that connects paracetamol molecules, as compared with pure paracetamol polymorphs. Pyridine is able to compete for a proton with a stronger proton acceptor – the acetamide group oxygen atom. This illustrates that a comparison of the strengths of individual H-bonds can be misleading when trying to predict crystal packing, since the total lattice energy is the result of an interplay between a multitude of interactions. This fact is of interest for understanding the pharmacological action of paracetamol, demonstrating that its phenol group can form H-bonds with N-atoms of heterocycles, even in the presence of other strongly competing proton acceptors. The possibility of forming infinite molecular chains linked by -NH…O=C- hydrogen bonds with void-filling pyridine molecules to optimise packing, can be suggested as a driving force for the exclusion of -OH…O=C- bond formation. The structure, however, is not stable on air and easily loses pyridine molecules to give the monoclinic polymorph of paracetamol.

Acknowledgements

The research was funded by the Russian Academy of Sciences and by the Ministry of Science and Education. Language polishing by Adam Michalchuk is appreciated.

Notes and references

[a]*Institute of Solid State Chemistry and Mechanochemistry SB RAS, 630128, Kutateladze Street 18, Novosibirsk, Russian Federation*
[b]*Novosibirsk State University, 630090, Pirogova Street 2, Novosibirsk, Russian Federation*
[c]*Nikolaev Institute of Inorganic Chemistry SB RAS, 630090, Pr. Ac. Lavrentyeva 3, Novosibirsk, Russian Federation*
[d]*Lavrentyev Institute of Hydrodynamics SB RAS,630090, Pr. Ac. Lavrentyeva 15, Novosibirsk, Russian Federation*
[e]*Budker Institute of Nuclear Physics SB RAS,630090, Pr. Ac. Lavrentyeva 11, Novosibirsk, Russian Federation*

† Electronic Supplementary Information (ESI) available: CIF's and checkCIF reports for *bis*(paracetamol) pyridine at different temperatures, 2-D synchrotron XRD patterns, discussion of the details of the choice of a model of phase diagram, details on crystal data, data collection and refinement, data on torsion angles and geometry of intermolecular hydrogen bonds at multiple temperatures, data on lattice strain on cooling. See DOI: 10.1039/b000000x/

1 T. K. Adalder and P. Dastidar, *Cryst. Growth Des.*, 2014, **14**, 2254–2262.
2 C. B. Aakeröy, T. K. Wijethunga and J. Desper, *J. Mol. Struct.*, 2014, **1072**, 20–27.
3 I. Matulková, J. Cihelka, M. Pojarová, K. Fejfarová, M. Dušek, I. Císařová, P. Vaněk, J. Kroupa, P. Němec, N. Tesařová and I. Němec, *CrystEngComm*, 2014, **16**, 1763–1776.
4 G. R. Desiraju, *J. Am. Chem. Soc.*, 2013, **135**, 9952–9967.
5 M. D. Eddleston, B. Patel, G. M. Day and W. Jones, *Cryst. Growth Des.*, 2013, **13**, 4599–4606.
6 O. Almarsson and M. J. Zaworotko, *Chem. Commun. (Camb).*, 2004, 1889–1896.
7 P. M. Bhatt, Y. Azim, T. S. Thakur and G. R. Desiraju, *Cryst. Growth Des.*, 2009, **9**, 951–957.
8 J. Ellena, M. D. Bocelli, S. B. Honorato, A. P. Ayala, A. C. Doriguetto and F. T. Martins, *Cryst. Growth Des.*, 2012, **12**, 5138–5147.
9 R. Thakuria, A. Delori, W. Jones, M. P. Lipert, L. Roy and N. Rodríguez-Hornedo, *Int. J. Pharm.*, 2013, **453**, 101–125.
10 D.-K. Bučar, S. Filip, M. Arhangelskis, G. O. Lloyd and W. Jones, *CrystEngComm*, 2013, **15**, 6289–6291.
11 W. Jones, W. D. S. Motherwell and A. V. Trask, *MRS Bull.*, 2006, **31**, 875–879.
12 D. Yan, A. Delori, G. O. Lloyd, T. Friščić, G. M. Day, W. Jones, J. Lu, M. Wei, D. G. Evans and X. Duan, *Angew. Chem. Int. Ed. Engl.*, 2011, **50**, 12483–12486.
13 T. Friščić and W. Jones, *J. Pharm. Pharmacol.*, 2010, **62**, 1547–1559.
14 S. G. Fleischman, S. S. Kuduva, J. A. McMahon, B. Moulton, R. D. Bailey Walsh, N. Rodríguez-Hornedo and M. J. Zaworotko, *Cryst. Growth Des.*, 2003, **3**, 909–919.
15 D. Cincić, T. Friscić and W. Jones, *Chemistry*, 2008, **14**, 747–753.
16 A. M. Moragues-Bartolome, W. Jones and A. J. Cruz-Cabeza, *CrystEngComm*, 2012, **14**, 2552–2559.
17 T. Friščić and W. Jones, *Faraday Discuss.*, 2007, **136**, 167–178.
18 M. Viertelhaus, R. Hilfiker, F. Blatter and M. Neuburger, *Cryst. Growth Des.*, 2009, **9**, 2220–2228.
19 R. Kaur, B. V. Lalithalakshmi and T. N. Guru Row, *Cryst. Growth Des.*, 2014, **14**, 2614–2620.
20 W. Beckmann, *Crystallization*, Wiley-VCH Verlag GmbH & Co. KGaA, Weinheim, Germany, 2013.

21 A. Chen, J. Zhu, K. Chen, B. Wu, L. Ji and Y. Wu, *Asia-Pacific J. Chem. Eng.*, 2013, **8**, 354–361.
22 M. Kikuchi, S. Iwabuchi, T. Kikkou, K. Noguchi, M. Odaka, M. Yohda, M. Kawata, C. Sato and O. Matsumoto, *Acta Crystallogr. Sect. F. Struct. Biol. Cryst. Commun.*, 2013, **69**, 942–945.
23 M. Le Page Mostefa, H. Muhr, E. Plasari and M. Fauconet, *Powder Technol.*, 2014, **255**, 98–102.
24 E. Temmel, S. Wloch, U. Müller, D. Grawe, R. Eilers, H. Lorenz and A. Seidel-Morgenstern, *Chem. Eng. Sci.*, 2013, **104**, 662–673.
25 S. J. Nehm, B. Rodríguez-Spong and N. Rodríguez-Hornedo, *Cryst. Growth Des.*, 2006, **6**, 592–600.
26 T. Rager and R. Hilfiker, *Cryst. Growth Des.*, 2010, **10**, 3237–3241.
27 T. Rager and R. Hilfiker, *Zeitschrift für Phys. Chemie*, 2009, 223, 793–813.
28 N. Rodríguez-Hornedo, S. J. Nehm, K. F. Seefeldt, Y. Pagán-Torres and C. J. Falkiewicz, *Mol. Pharm.*, 2006, **3**, 362–367.
29 M. D. Eddleston, M. Arhangelskis, T. Friščić and W. Jones, *Chem. Commun. (Camb).*, 2012, **48**, 11340–11342.
30 T. Friščič and W. Jones, *Cryst. Growth Des.*, 2009, **9**, 1621–1637.
31 T. Friščič and W. Jones, *Ann. Chim. Sci. des Matériaux*, 2009, **34**, 415–428.
32 K. Fucke, S. A. Myz, T. P. Shakhtshneider, E. V. Boldyreva and U. J. Griesser, *New J. Chem.*, 2012, **36**, 1969–1977.
33 S. A. Myz, T. P. Shakhtshneider, N. A. Tumanov and E. V. Boldyreva, *Russ. Chem. Bull.*, 2013, **61**, 1798–1809.
34 N. A. Tumanov, S. A. Myz, T. P. Shakhtshneider and E. V. Boldyreva, *CrystEngComm*, 2012, **14**, 305–313.
35 S. A. Myz, T. P. Shakhtshneider, K. Fucke, A. P. Fedotov, E. V. Boldyreva, V. V. Boldyrev and N. I. Kuleshova, *Mendeleev Commun.*, 2009, **19**, 272–274.
36 E. Boldyreva, *Chem. Soc. Rev.*, 2013, **42**, 7719–7738.
37 R. Hilfiker, *Crystallization*, Wiley-VCH Verlag GmbH & Co. KGaA, Weinheim, Germany, 2013.
38 G. Coquerel, *Chem. Soc. Rev.*, 2014, **43**, 2286–2300.
39 A. O. L. Evora, R. A. E. Castro, T. M. R. Maria, M. R. Silva, J. H. Ter Horst, J. Canotilho and M. E. S. Eusébio, *Int. J. Pharm.*, 2014, **466**, 68–75.
40 D. M. Croker, R. J. Davey, Å. C. Rasmuson and C. C. Seaton, *Cryst. Growth Des.*, 2013, **13**, 3754–3762.
41 S. Chen, H. Xi, R. F. Henry, I. Marsden and G. G. Z. Zhang, *CrystEngComm*, 2010, **12**, 1485–1493.
42 A. Alhalaweh and S. P. Velaga, *Cryst. Growth Des.*, 2010, **10**, 3302–3305.
43 H. Yamashita, Y. Hirakura, M. Yuda, T. Teramura and K. Terada, *Pharm. Res.*, 2013, **30**, 70–80.
44 G. Rothenberg, A. P. Downie, C. L. Raston and J. L. Scott, *J. Am. Chem. Soc.*, 2001, **123**, 8701–8708.
45 I. A. Tumanov, A. F. Achkasov, E. V. Boldyreva and V. V. Boldyrev, *CrystEngComm*, 2011, **13**, 2213–2216.
46 E. A. Losev and E. V. Boldyreva, *CrystEngComm*, 2014, **16**, 3857–3866.
47 E. A. Losev, M. A. Mikhailenko, A. F. Achkasov and E. V. Boldyreva, *New J. Chem.*, 2013, **37**, 1973–1981.
48 E. A. Losev, M. A. Mikhailenko and E. V. Boldyreva, *Dokl. Phys. Chem.*, 2011, **439**, 153–156.
49 E. V Boldyreva, V. A. Drebushchak, I. E. Paukov, Y. A. Kovalevskaya and T. N. Drebushchak, *J. Therm. Anal. Calorim.*, 2004, **77**, 607–623.
50 A. Łuczak, L. J. Jallo, R. N. Dave and Z. Iqbal, *Powder Technol.*, 2013, **236**, 52–62.
51 E. V. Boldyreva, T. P. Shakhtshneider, H. Ahsbahs, H. Sowa and H. Uchtmann, in *Journal of Thermal Analysis and Calorimetry*, 2002, vol. 68, pp. 437–452.
52 T. N. Drebushchak and E. V. Boldyreva, *Z. Krist.*, 2004, **219**, 506–512.
53 E. V. Boldyreva, T. P. Shakhtshneider, M. A. Vasilchenko, H. Ahsbahs and H. Uchtmann, *Acta Crystallogr. B.*, 2000, **56**, 299–309.
54 N. Tsapatsaris, S. Landsgesell, M. M. Koza, B. Frick, E. V. Boldyreva and H. N. Bordallo, *Chem. Phys.*, 2013, **427**, 124–128.
55 N. Tsapatsaris, B. A. Kolesov, J. Fischer, E. V Boldyreva, L. Daemen, J. Eckert and H. N. Bordallo, *Mol. Pharm.*, 2014, **11**, 1032–1041.
56 B. A. Kolesov, M. A. Mikhailenko and E. V Boldyreva, *Phys. Chem. Chem. Phys.*, 2011, **13**, 14243–14253.
57 C. C. Wilson, *Zeitschrift fur Krist.*, 2000, **215**, 693–701.
58 C. D. Pathak, K. T. Savjani, A. K. Gajjar and J. K. Savjani, *Int. J. Pharm. Pharm. Sci.*, 2013, **5**, 414–419.
59 M. A. Elbagerma, H. G. M. Edwards, T. Munshi and I. J. Scowen, *CrystEngComm*, 2011, **13**, 1877–1884.
60 S. Karki, T. Friščić, . Fabián, P. R. Laity, G. M. Day and W. Jones, *Adv. Mater.*, 2009, **21**, 3905–3909.
61 V. André, M. F. M. da Piedade and M. T. Duarte, *CrystEngComm*, 2012, **14**, 5005–5014.
62 J. A. Hayes, K. S. Eccles, S. E. Lawrence and H. A. Moynihan, *Carbohydr. Res.*, 2012, **349**, 108–112.
63 I. D. H. Oswald, I. Chataigner, S. Elphick, F. P. A. Fabbiani, A. R. Lennie, J. Maddaluno, W. G. Marshall, T. J. Prior, C. R. Pulham and R. I. Smith, *CrystEngComm*, 2009, **11**, 359–366.
64 F. P. A. Fabbiani, D. R. Allan, A. Dawson, W. I. F. David, P. A. McGregor, I. D. H. Oswald, S. Parsons and C. R. Pulham, *Chem. Commun.*, 2003, **9**, 3004–3005.
65 R. M. Vrcelj, N. I. B. Clark, A. R. Kennedy, D. B. Sheen, E. E. A. Shepherd and J. N. Sherwood, *J. Pharm. Sci.*, 2003, **92**, 2069–2073.
66 P. A. McGregor, D. R. Allan, S. Parsons and C. R. Pulham, *J. Pharm. Sci.*, 2002, **91**, 1308–1311.
67 F. H. Allen, *Acta Crystallogr. Sect. B Struct. Sci.*, 2002, **58**, 380–388.
68 M. A. Mikhailenko, T. N. Drebushchak, T. P. Shakhtsneider and V. V. Boldyrev, *Arkivoc*, 2005, **2004**, 156–169.
69 R. V Shchepin, W. Liu, H. Yin, I. Zagol-Ikapitte, T. Amin, B.-S. Jeong, L. J. Roberts, J. A. Oates, N. A. Porter and O. Boutaud, *ACS Med. Chem. Lett.*, 2013, **4**, 710–714.
70 T.-G. Nam, S. J. Nara, I. Zagol-Ikapitte, T. Cooper, L. Valgimigli, J. A. Oates, N. A. Porter, O. Boutaud and D. A. Pratt, *Org. Biomol. Chem.*, 2009, **7**, 5103–5112.
71 C. Drahl, *Chem. Eng. News*, **92**, 31–32.
72 N. V Surovtsev, S. V Adichtchev, V. K. Malinovsky, A. G. Ogienko, V. A. Drebushchak, A. Y. Manakov, A. I. Ancharov, A. S. Yunoshev and E. V Boldyreva, *J. Chem. Phys.*, 2012, **137**, 065103.
73 I. G. Binev, P. Vassileva-Boyadjieva and Y. I. Binev, *J. Mol. Struct.*, 1998, **447**, 235–246.
74 E. V. Boldyreva, T. P. Shakhtshneider, H. Ahsbahs, H. Uchtmann, E. B. Burgina and V. P. Baltakhinov, *Pol. J. Chem.*, 2002, **76**, 1333–1346.
75 A. J. Cruz-Cabeza and J. Bernstein, *Chem. Rev.*, 2014, **114**, 2170–2191.
76 B. H. Torrie, S.-X. Weng and B. M. Powell, *Mol. Phys.*, 1989, **67**, 575–581.
77 D. R. Allan and S. J. Clark, *Phys. Rev. B - Condens. Matter Mater. Phys.*, 1999, 60, 6328–6334.
78 T. J. Kistenmacher, G. A. Rand and R. E. Marsh, *Acta Crystallogr. Sect. B Struct. Crystallogr. Cryst. Chem.*, 1974, **30**, 2573–2578.
79 I. D. H. Oswald, D. R. Allan, P. A. McGregor, W. D. S. Motherwell, S. Parsons and C. R. Pulham, *Acta Crystallogr. Sect. B Struct. Sci.*, 2002, **58**, 1057–1066.
80 J. R. G. Sander, D.-K. Bučar, R. F. Henry, B. N. Giangiorgi, G. G. Z. Zhang and L. R. MacGillivray, *CrystEngComm*, 2013, **15**, 4816–4822.
81 V. K. Srirambhatla, A. Kraft, S. Watt and A. V. Powell, *Cryst. Growth Des.*, 2012, **12**, 4870–4879.
82 A. R. Ubellohde, *Proceed. R. Soc. London Ser. A.*, 1939, **173**, 417–427.
83 K. J. Gallagher, A. R. Ubbelohde and I. Woodward, *Acta Crystallogr.*, 1955, **8**, 561–566.
84 K. Lonsdale, *Z. Krist.*, 1959, **112**, 188–212.

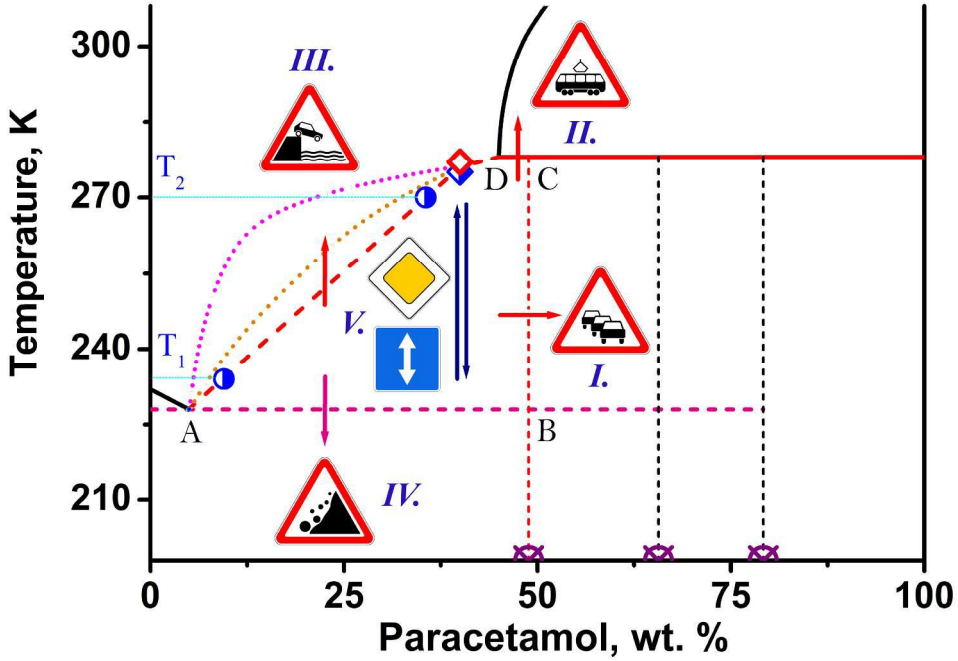

254x179mm (300 x 300 DPI)